Effects of Membrane Thickness on the Molecular Dynamics and Enzymatic Activity of Reconstituted Ca-ATPase†

Răzvan L. Cornea and David D. Thomas*

Department of Biochemistry, University of Minnesota Medical School, Minneapolis, Minnesota 55455

Received September 3, 1993; Revised Manuscript Received December 20, 1993®

ABSTRACT: We have studied the effect of phospholipid chain length on the activity and molecular dynamics of reconstituted Ca-ATPase from skeletal sarcoplasmic reticulum (SR), using time-resolved phosphorescence anisotropy (TPA) and electron paramagnetic resonance (EPR). We used reconstituted Ca-ATPase in exogenous phosphatidylcholines with monounsaturated chains 14–24 carbons long, to determine their effects on the physical properties of the Ca-ATPase and to correlate these physical changes with changes in the ATPase activity. In agreement with previous studies, we found that the enzymatic activity was maximal with a chain length of 18 and decreased substantially with longer or shorter chains. Our TPA results show that chain lengths longer or shorter than the optimal 18 result in a significantly decreased mobility of the Ca-ATPase, indicated by higher residual anisotropy and suggesting extensive protein aggregation. Saturation-transfer EPR data obtained with a spin label bound to a different site also indicates substantial immobilization of the enzyme, supporting the TPA results. There is good agreement between the fractional inhibition of the Ca-ATPase activity and the fraction of the enzyme in large aggregates. Solubilization in the nonionic detergent $C_{12}E_8$ demonstrated that inhibition of enzyme activity is reversible. In contrast to the large effects on protein mobility, these changes in chain length had little or no effect on hydrocarbon chain mobility as detected by conventional EPR at different depths in the membrane. We conclude that the Ca-ATPase has an optimum lipid bilayer thickness, presumably matching the thickness of the hydrophobic transmembrane surface of the enzyme, and that deviation from this optimum thickness produces a hydrophobic mismatch that induces protein aggregation and hence Ca-ATPase inhibition. This is consistent with our proposal that protein dynamics and protein–protein interactions are of primary importance to the Ca-ATPase mechanism.

Integral membrane proteins fulfill their role in a highly organized environment that is dominated by phospholipid. Although often regarded as a passive cell envelope or an inert anchor place for membrane proteins, the phospholipid bilayer plays an important role in regulating many membrane functions. In particular, it appears that the hydrocarbon chain structure and dynamics can modulate the conformation state of integral membrane proteins as well as their lateral distribution in the membrane. Theoretical models (Owicki et al., 1978; Mouritsen & Bloom, 1984; Sperotto & Mouritsen, 1991) and experimental approaches (Lewis & Engelman, 1983a; Ryba & Marsh, 1992) have suggested that hydrophobic mismatch between the hydrophobic thickness of the bilayer (d_l) and the transmembrane span of the protein (d_p) (Figure 1), causes *aggregation* of proteins within the membrane. Altering the thickness of the phospholipid environment of an integral membrane protein has also been shown to have a profound *functional* effect in a variety of membrane systems (Johannsson et al., 1981a,b; Lee, 1991; In't Veld et al., 1991; Montecucco et al., 1982; Criado et al., 1984). However, a direct relationship between hydrophobic mismatch-induced protein aggregation and biological function has only limited support from experimental evidence.

Understanding the correlation of molecular dynamics and enzymatic activity within a biological membrane is extremely important in assembling an accurate model describing the overall functioning of the membrane system. Skeletal muscle sarcoplasmic reticulum (SR)[1] membranes have been the target of intensive research devoted to understanding precisely how

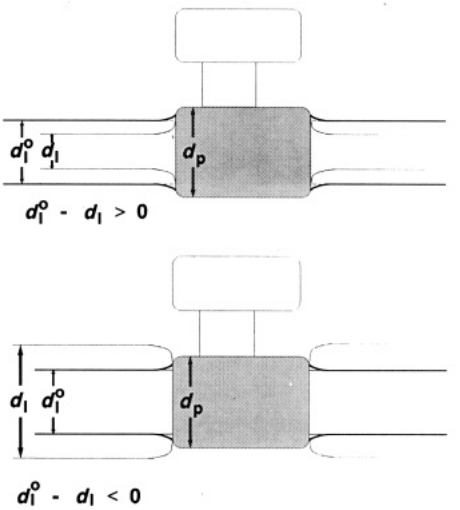

FIGURE 1: There is proposed to be an optimal bilayer thickness (d_l^0) required by an integral membrane protein of hydrophobic thickness (d_p) for its normal function and degree of aggregation.

the motions and the interactions of the SR Ca-ATPase (the enzyme responsible for the active transport of calcium in

† This work was supported by NIH Grant GM27906 to D.D.T.
* To whom correspondence should be addressed.
® Abstract published in *Advance ACS Abstracts,* February 1, 1994.

[1] Abbreviations: SR, sarcoplasmic reticulum; TPA, transient phosphorescence anisotropy; EPR, electron paramagnetic resonance; ST-EPR saturation transfer electron paramagnetic resonance; ErITC, erythrosin-5-isothiocyanate; MSL, maleimide spin label; n-SASL, stearic acid spin label; PC, phosphatidylcholine; ATP, adenosine triphosphate; $C_{12}E_8$, octaethylene glycol dodecyl ether; MOPS, 3-(*N*-morpholino)propanesulfonic acid; DMF, *N*,*N*-dimethylformamide; NADH, β-nicotinamide adenine dinucleotide, reduced form; TPX, tetramethylene polymer plastic; BSA, bovine serum albumin; NEM, *N*-ethylmaleimide; IU, international units.

0006-2960/94/0433-2912$04.50/0

muscle) and its surrounding lipids affect its enzymatic activity [reviewed by Thomas and Mahaney (1993)]. We have chosen the SR Ca-ATPase for the present study, not only to provide a better understanding of calcium regulation in muscle, but also because this is one of the best characterized integral membrane enzymes, serving as a model for the biochemistry and biophysics of active transport and other membrane-based energy transductions.

A variety of perturbations have been used to alter the physical state of the protein and of the bilayer in order to correlate the molecular dynamics of the enzyme and its associated lipids with Ca-ATPase functioning. Saturation transfer EPR (ST-EPR) spectroscopy, which is optimally sensitive to motions on the microsecond time scale, was used to monitor the global rotational diffusion of the Ca-ATPase under various circumstances affecting the lateral aggregation of the enzyme, e.g., (a) decreasing temperature (Bigelow et al., 1986; Squier et al., 1988b; Birmachu & Thomas, 1990), (b) selectively cross-linking the Ca-ATPase (Squier et al., 1988a), (c) decreasing the lipid/protein ratio (Squier & Thomas, 1988), or (d) crystallizing the ATPase by using vanadate (Lewis & Thomas, 1986). It has been determined that conditions favoring increased protein aggregation have a profound inhibitory effect on both ATP hydrolysis and calcium uptake by SR. Increased Ca-ATPase rotation (as detected by ST-EPR) due to increased lipid fluidity (as detected by conventional EPR) resulted in a concomitant increase in Ca-ATPase activity (Bigelow & Thomas, 1987). As an alternative to ST-EPR, phosphorescent probes have also been used to measure microsecond–millisecond protein rotations, using time-resolved phosphorescence anisotropy (TPA). With TPA, probe populations with different rates of motion can be resolved as distinct exponential decay components (characterized by rotational correlation times ϕ_i) that are directly related to rotational amplitudes and mole fractions, generally leading to a less model-dependent interpretation of data relative to ST-EPR (Thomas, 1986). TPA measurements of the Ca-ATPase also show a strong correlation between conditions that inhibit the Ca-ATPase and those that promote protein association (Birmachu & Thomas, 1990; Voss et al., 1991; Karon & Thomas, 1993). The results of all these studies indicated that optimal Ca-ATPase enzymatic function correlates directly with the ability of the Ca-ATPase to undergo microsecond rotational motion in a fluid lipid bilayer. Notably, the primary physical effect evidenced by the TPA studies is not a change in a rate but a change in the equilibrium constant for protein–protein association.

Previous studies have established that the ATP-hydrolysis activity of reconstituted Ca-ATPase is sensitive to the hydrocarbon chain length of the phospholipid, with an optimal length of 18–20 carbons [Johannsson, 1981a; reviewed by Lee (1991)]. Extreme bilayer thicknesses have also been shown to perturb the stoichiometry of calcium binding to Ca-ATPase (Starling et al., 1993) and affect its conformational equilibrium, as suggested by the fluorescence response of the fluorescein isothiocyanate-labeled Ca-ATPase (Froud et al., 1986). Munkonge et al. (1988) showed that a suboptimal bilayer thickness resulted in increased fluorescence energy transfer between Ca-ATPase molecules. However there have been no studies of the effects of hydrophobic mismatch on protein dynamics in SR.

Therefore, in the present study, we have used TPA and ST-EPR to compare the microsecond protein rotational motion of the SR Ca-ATPase reconstituted in bilayers of various hydrophobic thicknesses. The possible involvement of phospholipid chain order parameter was investigated by conventional EPR. The result is a quantitative correlation of physical effects with the biological function, as affected by hydrophobic mismatch.

MATERIALS AND METHODS

Reagents and Solutions. Erythrosin-5-isothiocyanate (ErITC) was obtained from Molecular Probes, Inc. (Eugene, OR). The spin labels were purchased from Aldrich. All labels were stored in DMF at −70 °C. ATP, $C_{12}E_8$, lactate dehydrogenase, pyruvate kinase, MOPS, and NADH were obtained from Sigma. Phosphoenolpyruvate was purchased from Boehringer Mannheim. All other reagents were obtained from Mallinckrodt and were of the highest purity available. All enzymatic assays and spectroscopy experiments were carried out at 37 °C in a buffer containing 60 mM KCl, 6 mM $MgCl_2$, 0.1 mM $CaCl_2$, and 25 mM MOPS, pH 7.0 (henceforth denoted as experimental buffer).

Unless otherwise noted, all preparations were executed at 0–4 °C. Sarcoplasmic reticulum vesicles were prepared from New Zealand White rabbit fast skeletal muscle as described previously (Fernandez et al., 1980). Purified, partially delipidated Ca-ATPase was prepared essentially as described by East and Lee (1982) and stored in 0.25 M sucrose, 1 M KCl, and 50 mM potassium phosphate, pH 8.0 (henceforth denoted as buffer A), in 2-mg aliquots (a minimum of 30 mg/mL) at −70 °C.

Assays. Calcium-dependent ATP hydrolysis activity was determined with an enzyme-coupled assay in a medium containing 60 mM KCl, 6 mM $MgCl_2$, 25 mM MOPS (ph 7.0), 0.1 mM $CaCl_2$, 0.15 mM NADH, 0.42 mM phosphoenolpyruvate, 7.5 IU of pyruvate kinase, 19 IU of lactate dehydrogenase, and 2.1 mM ATP, in a total volume of 1 mL. The assay was started by the addition of 5 μg (10 μL) of reconstituted ATPase to the assay cuvette. Protein concentrations were determined by the biuret assay (Gornall et al., 1949) using bovine serum albumin as standard. The molar concentration of lipids in the purified and reconstituted Ca-ATPase preparations was determined from phosphorus assays (Chen et al., 1956).

Reconstitution. The purified Ca-ATPase was reconstituted in exogenous monounsaturated phosphatidylcholines with hydrocarbon chains 14–24 carbons long. We used the reconstitution procedure described by Froud et al. (1986), with slight modifications. For each lipid species tested, 20 μmol of the lipid was dried with a flow of nitrogen and lyophilized overnight. The lipid sample was rehydrated in 0.8 mL of 12 mg/mL cholate in buffer A, for about 1 h, in closed 1-mL Eppendorf tubes, under N_2, with frequent vortexing. The sample was then sonicated in a bath sonicator (Laboratory Supplies Co., Inc., Model G112SP1T), for 5 min at 25 °C. Purified Ca-ATPase (2 mg) was added to each lipid–cholate mixture and allowed to equilibrate for 1 h at 5 °C for chain lengths 14–20 and for 20 min at 5 °C, followed by 40 min at 25 °C, for chain lengths 22–24. For ATPase activity measurements, a small portion of each sample was diluted 5 times in buffer A and stored on ice. The remaining sample was washed three times in buffer A [for MSL labeling the final wash was in 0.3 M sucrose and 20 mM MOPS, pH 7.0 (henceforth denoted as sucrose buffer)] by centrifuging at 65000*g* for 10 min in 3.5-mL polycarbonate tubes in a Beckman TL-100 centrifuge. The pellets were resuspended in buffer A to 2 mg/mL for ErITC labeling and in sucrose buffer to 10 mg/mL for MSL labeling.

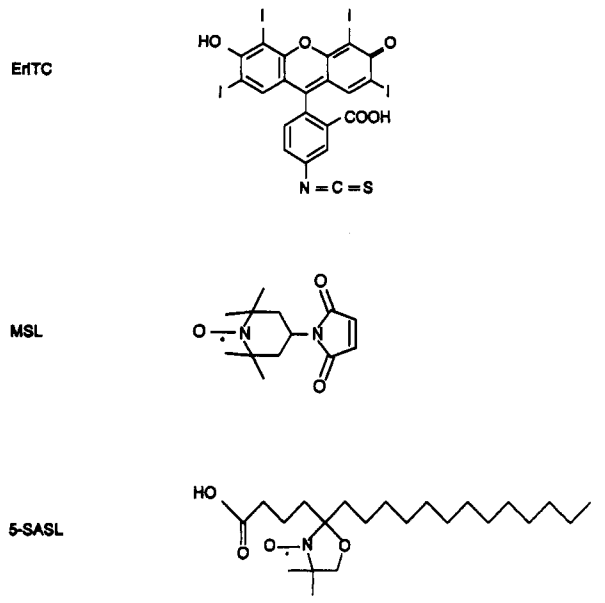

FIGURE 2: Labels used in this study. The Ca-ATPase was specifically labeled on Lys_{515} with the phosphorescent label ErITC (erythrosin 5-isothiocyanate). MSL [maleimide spin label, *N*-(1-oxyl-2,2,6,6-tetramethyl-4-piperidinyl)maleimide] was covalently bound to the Ca-ATPase for ST-EPR measurements of the enzyme's microsecond rotational motion. 5-, 9-, 14-, and 16-SASL (stearic acid spin label), *N*-oxyl-4',4'-dimethyloxazolidine derivatives of stearic acid, were incorporated noncovalently into protein-free PC vesicles for conventional EPR measurements of hydrocarbon chain dynamics at various depths in the bilayer (5-SASL is represented here).

ErITC Labeling. The Ca-ATPase was specifically labeled at Lys_{515} with the phosphorescent dye ErITC (Figure 2), essentially as described by Birmachu and Thomas (1990). The reconstituted Ca-ATPase (2 mg/mL) was incubated with 20 μM ErITC for 30 min at 25 °C. At the end of this reaction time, the samples were diluted 6-fold with buffer A containing 1 mg/mL BSA and incubated 20 min at 4 °C prior to pelleting the membranes by centrifugation at 65000*g* for 20 min. The incubation with BSA ensured the removal of noncovalently bound label. The pellets were washed once more in buffer A and resuspended in experimental buffer to a concentration of 6–8 mg/mL. The phosphorescence samples were prepared by diluting the ErITC-labeled Ca-ATPase to 0.1–0.4 mg/mL in experimental buffer. Prior to data collection the phosphorescence samples were enzymatically deoxygenated according to the method of Eads et al. (1984) by adding 100 μg/mL glucose oxidase, 15 μg/mL catalase, and 5 mg/mL glucose. Deoxygenation was carried out for 15 min prior to data collection, in sealed cuvettes (0.2 × 1 cm), at the experimental temperature.

Spin Labeling. For ST-EPR spectroscopy the Ca-ATPase was labeled at cysteines 344 and 364 (Bigelow & Inesi, 1991) with the short-chain maleimide spin label *N*-(1-oxyl-2,2,6,6-tetramethyl-4-piperidinyl)maleimide (MSL; Figure 2) covalently bound to the purified enzyme essentially according to the method of Thomas and Hidalgo (1978) [modified by Bigelow et al. (1986)]. *N*-Ethylmaleimide (NEM) was first added at a ratio of 1.0 mol/10^5 g of protein to the reconstituted Ca-ATPase (10 mg/mL) to block fast-reacting sulfhydryl groups. After incubation for 30 min at 25 °C, MSL was added at a ratio of 2.5 mol/10^5 g of protein and incubated 50 min at 25 °C. The reaction was stopped by 8-fold dilution into cold sucrose buffer and the membranes were washed three times by centrifuging at 65000*g* for 10 min at 3.5-mL polycarbonate tubes in a Beckman TL-100 centrifuge.

Lipid hydrocarbon chain rotational mobility was measured by EPR in protein-free bilayers containing stearic acid spin labels (designated n-SASL), which are *N*-oxyl-4',4'-dimethyloxazolidine derivatives of stearic acid (Figure 2). Incorporation of the spin label into protein-free lipid samples (aqueous dispersions) was accomplished by adding the spin label (from a 25 mM stock in DMF) to aliquots of PC (in chloroform) at a ratio of 1 label:200 lipids. The mixtures were freeze-dried overnight and rehydrated in experimental buffer under frequent vortexing. Each sample was sonicated (same equipment as above) at 25 °C for 5 min prior to EPR spectra acquisition. The lipid concentrations were sufficiently high (64 μM) to minimize the spectral contribution from unbound, aqueous labels.

Spectroscopic Instrumentation. The instrumentation for time-resolved phosphorescence was described in detail previously (Ludescher & Thomas, 1988). The phosphorescence anisotropy decay is given by

$$r(t) = \frac{I_{\parallel}(t) - GI_{\perp}(t)}{I_{\parallel}(t) + 2GI_{\perp}(t)} \quad (1)$$

where $I_{\parallel}(t)$ and $I_{\perp}(t)$ were obtained by signal-averaging the time-dependent phosphorescence decays with a single detector and a polarizer that alternates between the vertical ($I_{\parallel}$) and horizontal ($I_{\perp}$) positions every 2000 laser pulses. The laser repetition rate was 100 Hz, so a typical $r(t)$ acquisition required about 7 min to complete 10 loops, or cycles, of 4000 laser pulses each (2000 in each orientation). G is an instrumental correction factor, determined by measuring the anisotropy of free dye in solution under experimental conditions.

EPR spectra were acquired using a Bruker ESP-300 spectrometer equipped with a Bruker E4201 cavity and digitized with the spectrometer's built-in microcomputer using Bruker OS-9-compatible ESP 1620 spectral acquisition software. Spectra were downloaded to an IBM-compatible microcomputer and analyzed using software developed in our laboratory by R. L. H. Bennett. Conventional (V_1) EPR was used to detect submicrosecond motions of the lipid spin labels, and saturation transfer EPR (ST-EPR, V'_2) was used to detect the submillisecond motions of the reconstituted MSL-Ca-ATPase. V_1 spectra were obtained using 100-kHz field modulation (with a peak-to-peak modulation amplitude of 2 G), with a microwave field intensity (H_1) of 0.032 G for MSL-Ca-ATPase and 0.14 G for SASL. V'_2 spectra of the MSL-Ca-ATPase were obtained with 50-kHz field modulation (with a peak-to-peak amplitude of 5 G), with a microwave field intensity of 0.25 G. Lipid spin-labeled samples were contained in glass capillaries, whereas maleimide spin-labeled Ca-ATPase samples were contained in gas-permeable capillaries made of TPX (Popp & Hyde, 1981), allowing the removal of dissolved oxygen by purging the samples with N_2 (Squire & Thomas, 1986). Sample temperature was controlled to within 0.5 °C with a Bruker ER 4111 variable-temperature controller. Sample temperature was monitored with a Sensortek Bat-21 digital thermometer using an IT-21 thermocouple probe inserted into the top of the sample capillary, such that it did not interfere with spectral acquisition.

Analysis of TPA Data. It has been shown previously (Birmachu & Thomas, 1990) that the TPA of ErITC-SR is dominated by the uniaxial rotational diffusion of the labeled Ca-ATPase about an axis normal to the bilayer. In theory, this should result in a biexponential anisotropy decay component for each distinct rotating species [Kinosita et al., 1984; reviewed by Thomas (1986)], but Birmachu and Thomas

(1990) have shown that, for ErITC-SR, only one of the two exponentials contributes significantly, and the TPA decay is described accurately by

$$\frac{r(t)}{r_0} = \sum_{i=1}^{n} A_i \exp(-t/\phi_i) + A_\infty \quad (2)$$

where ϕ_i is the rotational correlation time (inversely proportional to the rotational diffusion coefficient D_{mi} for a given rotating species), A_i are the normalized amplitudes (r_i/r_0), r_0 is the initial anisotropy [$r(0) = r_0 = \sum r_i + r_\infty$]. A_∞ is the normalized residual anisotropy (r_∞/r_0)

$$A_\infty = A_{\infty 0} + f_I(1 - A_{\infty 0}) \quad (3)$$

where f_I is the fraction of proteins that are immobile on the observed time scale and $A_{\infty 0}$ is the residual anisotropy of a reference sample for which $f_I = 0$ (see Discussion) and describes the extent to which the probe's motion is restricted in angular amplitude, due to the fixed angles θ_{ma} and θ_{me} of the probe's absorption transition moment relative to the membrane normal and the probe's emission transition moment relative to the membrane normal, respectively:

$$A_{\infty 0} = \frac{P_2(\cos^2 \theta_{ma})\, P_2(\cos^2 \theta_{me})}{P_2(\cos^2 \theta_{ae})} \quad (4)$$

where $P_2(\chi) = (3\chi^2 - 1)/2$ and θ_{ae} is the angle between the absorption and emission transition dipoles (Lipari & Szabo, 1980).

The fraction of probes with a correlation time ϕ_i is thus given by $f_i = A_i/(1 - A_{\infty 0})$.

EPR Spectral Analysis. ST-EPR spectra of MSL-Ca-ATPase in SR were analyzed using the $V'_2\, H''/H$ line shape parameter (Squier & Thomas, 1986). Effective rotational correlation times (τ_r) in SR were determined from a standard curve constructed from an isotropically tumbling model system (Squier & Thomas, 1986). The protein rotational mobility, calculated as the inverse of the rotational correlation time, provides a parameter proportional to the rotational diffusion coefficient and lipid fluidity (Squier et al., 1988b; discussed below).

Fatty acid spin label EPR spectra were analyzed by measuring the inner ($2T'_\parallel$) and outer ($2T'_\perp$) spectral splittings, which are sensitive mainly to the rotational amplitude of hydrocarbon chain wobble relative to the membrane normal. The effective order parameter (S) was calculated from the splittings in two essentially equivalent ways. First, spectra having well-resolved extrema (S greater than 0.3), so that both $2T'_\parallel$ and $2T'_\perp$ could be measured, were analyzed according to Gaffney (1976):

$$S = \frac{T'_\parallel - (T'_\perp + C)}{T'_\parallel + 2(T'_\perp + C)}(1.66) \quad (5)$$

where $C = 1.4 - 0.053(2T'_\parallel - 2T'_\perp)$ and $2T'_\parallel$ and $2T'_\perp$ are the measured splittings between the inner and outer extrema resolved in the EPR spectrum. For 16-SASL spectra, (where S was always less than 0.3), eq 5 was not valid for calculating the effective order parameter (Squier et al., 1988b). Therefore, 16-SASL order parameters were determined by the expression (Gaffney, 1976)

$$S = \frac{T_0 - T'_\perp}{T_0 - T_\perp} \quad (6)$$

where T_0 is the isotropic hyperfine splitting constant in the absence of anisotropic effects and $T_\perp$ is the minimum value of the effective hyperfine tensor for an axially symmetric system (e.g., a lipid bilayer). The values of T_0 and $T_\perp$ used in this study were 14.3 ± 0.2 and 6.3 ± 0.3 G, respectively, as previously determined by Squier and Thomas (1989). The order parameter calculated from eq 5 or 6 can be used to calculate the effective lipid fluidity (inverse of viscosity, η), on the basis of empirical calibration plots obtained by Squier et al. (1988b).

Theory of Membrane Protein Rotational Diffusion. The rotational correlation time for uniaxial rotation of a cylindrical membrane particle (e.g., individual protein or protein aggregate) (ϕ_i in eq 2) can be expressed as a function of the membrane lipid viscosity (η), temperature (T), and the effective radius (a) of the portion of the protein in the bilayer (Saffman & Delbrück, 1975:

$$D_{mi} = \frac{kT}{(4\pi a^2 h\eta)} = \frac{1}{\phi_i} \quad (7)$$

where h is the thickness of the hydrocarbon phase of the lipid bilayer. Thus the protein rotational mobility ($1/\phi_i$, which = D_{mi} for ErITC-SR) should be proportional to the lipid fluidity (T/η; Squier et al., 1988b) and inversely proportional to the intramembrane area (πa^2) of the rotating protein and to the bilayer thickness. This theory relating protein size and lipid fluidity to protein rotational mobility is supported by previous studies on the Ca-ATPase, as measured by either ST-EPR (Squier et al., 1988a,b) or phosphorescence anisotropy (Birmachu & Thomas, 1990). Therefore, the effective radius (a) of the Ca-ATPase can be determined from the phosphorescence data if the lipid viscosity η and h are known. A substantial change in the effective radius is almost certainly due to protein association (aggregation) in the plane of the membrane. Thus the mole fraction f_i of proteins in a given oligomeric state can be calculated from A_i, as described above.

RESULTS

Effect of Bilayer Thickness on Ca-ATPase Rotational Motion, Measured by Phosphorescence Anisotropy. We used the erythrosin isothiocyanate phosphorescent probe (Figure 2), covalently attached to Lys_{515} of the Ca-ATPase, to observe the microsecond rotational motion of the reconstituted enzyme by TPA as a function of bilayer thickness. The TPA decays of the reconstituted ErITC-labeled Ca-ATPase show that the normalized anisotropy is increased (rotational mobility decreased) if the chain length is made either shorter or longer than 18 carbons (Figure 3). The most obvious effect is an increase in the anisotropy remaining at long times, which can be quantitated by determining the normalized residual anisotropy (A_∞) from the fits to eq 2. The anisotropy parameters calculated from the three-exponential fits, at the various phospholipid chain lengths, are listed in Table 1 and plotted in Figure 4. The clearest trend is in the residual anisotropy A_∞, which has been shown to be an accurate indicator of large-scale aggregation of the Ca-ATPase in the plane of the membrane (Voss et al., 1991). The lowest A_∞ (highest mobility) is supported by di(18:1)PC, while shorter or longer chains caused a gradual increase of A_∞, relative to the 18-carbon species. For the shortest (14) and longest (24) hydrocarbon lengths, we detected a dramatic, almost complete immobilization of the probe in the microsecond time range. The effect of bilayer thickness on the TPA decays is clearly consistent with a model in which the hydrophobic mismatch

Table 1: Phosphorescence Anisotropy Decay Parameters of Reconstituted ErITC-Labeled Ca-ATPase[a]

chain length	ϕ_1 (μS)	ϕ_2 (μS)	ϕ_3 (μS)	A_1	A_2	A_3	A_∞	r_0	$\langle\tau\rangle$ (μS)
14	5.6 (1.8)	123 (120)	452 (380)	0.130 (0.082)	0.040 (0.141)	−0.016 (0.169)	0.886 (0.170)	0.086 (0.024)	125.9 (19.6)
16	4.8 (2.0)	32 (20)	96 (110)	0.196 (0.108)	0.037 (0.120)	0.111 (0.117)	0.638 (0.064)	0.082 (0.02)	91.5 (10.8)
18	6.5 (2.2)	27 (10)	170 (40)	0.142 (0.042)	0.206 (0.025)	0.231 (0.038)	0.427 (0.025)	0.094 (0.01)	106.3 (24.4)
20	9.8 (2.1)	52 (40)	175 (30)	0.121 (0.033)	0.091 (0.024)	0.266 (0.044)	0.519 (0.040)	0.095 (0.006)	125.6 (18.5)
22	9.2 (2.2)	68 (50)	212 (60)	0.069 (0.035)	0.044 (0.048)	0.221 (0.052)	0.686 (0.034)	0.12 (0.03)	139.4 (2.9)
24	6.8 (1.5)	93 (40)	193 (140)	0.104 (0.014)	0.068 (0.028)	0.003 (0.031)	0.828 (0.028)	0.11 (0.02)	116.6 (3.2)

[a] Phosphorescence anisotropy decay parameters obtained from a nonlinear least-squares analysis (parameters defined as in eq 2, with $n = 3$) of phosphorescence anisotropy decays of reconstituted ErITC-labeled Ca-ATPase with exogenous phosphatidylcholines with chain lengths ranging from 14 to 24 carbons. $\langle\tau\rangle = \sum a_i\tau_i$ is the average lifetime of the intensity decay fit to

$$I(t) = \sum_{i=1}^{n} a_i \exp(-t/\tau_i) \tag{8}$$

with $n = 4$. Each value in the table is the average from eight experiments on three separate preparations, with the standard deviation in parentheses.

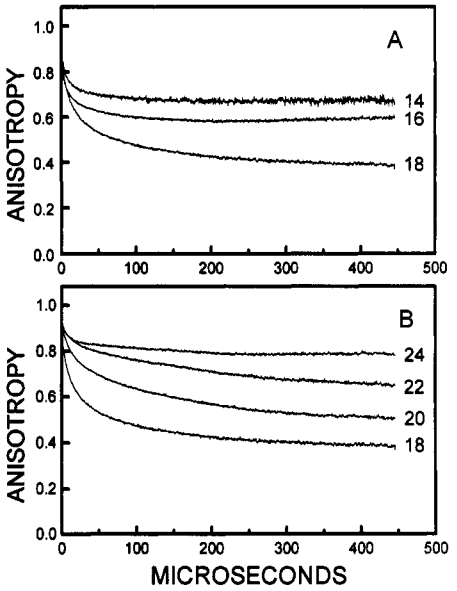

FIGURE 3: Normalized phosphorescence anisotropy decays $[r(t)/r_0]$ of ErITC-labeled Ca-ATPase reconstituted in di(n:1)PCs, with n ranging from 14 to 18 (A) and from 18 to 24 (B), at 37 °C. Values displayed at right edge represent chain lengths of the phosphatidylcholines utilized in reconstitution.

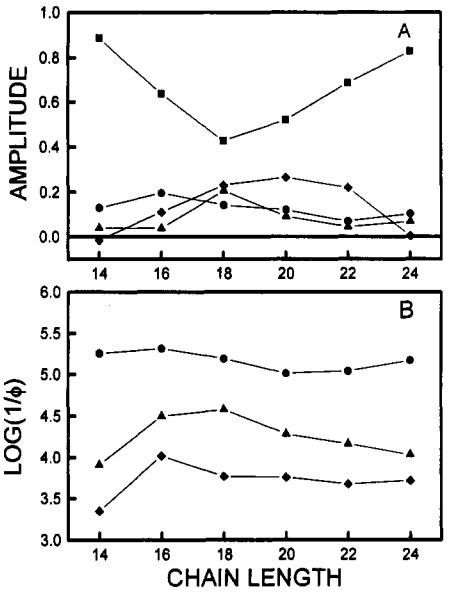

FIGURE 4: Effect of chain length on (A) the normalized phosphorescence anisotropy amplitudes A_1 (●), A_2 (▲), A_3 (◆), and A_∞ (■) and (B) on correlation times ϕ_1 (●), ϕ_2 (▲), and ϕ_3 (◆) from a three-exponential fit (eq 2) of data like that in Figure 3. Values are averaged over eight experiments.

between the lipid and the protein causes an increase in the mole fraction of immobile species, f_I (eq 3).

Effect of Bilayer Thickness on Ca-ATPase Rotational Motion, Measured by ST-EPR. The Ca-ATPase was covalently labeled at a different site with the maleimide spin label (MSL) and reconstituted in 18- and 24-carbon phosphatidylcholines. ST-EPR was employed to observe the effect of large hydrophobic mismatch on the overall rotational motion of the enzyme. Conventional (V_1) EPR and ST-EPR (V'_2) spectra of the reconstituted MSL-Ca-ATPase are shown in Figure 5. No change was detected in the V_1 spectra, as shown by the virtually unchanged values of the outer splitting, $2T'_\parallel$ (65.6 ± 0.3 G). In contrast, the V'_2 spectra, which report the overall rotational motion of the MSL-Ca-ATPase (Lewis & Thomas, 1986; Squier et al., 1988a), are very sensitive to the change in bilayer thickness (Figure 5). The effective correlation times observed for the 24-carbon reconstitution show a 5-fold increase relative to the 18-carbon control (Table 2), indicating substantial inhibition of the Ca-ATPase rotational motion, in agreement with the TPA data.

Phospholipid Chain Dynamics, Measured by Conventional EPR. The phospholipid hydrophobic chain dynamics was measured by EPR in protein-free phospholipid bilayers treated with stearic acid spin labels (SASL, Figure 2). 5-, 9-, 14-, and 16-SASL were used to measure the lipid order parmater at various depths in the bilayer. For example, 5-SASL was used to measure chain dynamics near the headgroup region, while 16-SASL was used to measure the order parameter deeper in the hydrophobic region. All four labels displayed a monotonic increase in their order parameters with increasing bilayer thickness (Figure 6). The effect of bilayer thickness on the order parameter reflects the fact that, as the chain becomes longer, a given label is at a longer distance from the bilayer's median lamella (where the chains tend to be more disordered) and relatively closer to the headgroup (where chain motion is more restricted), such that the label is simply reporting changes in order relative to the headgroup region, rather than an overall increased lipid order in thicker membranes. While this result complicates the interpretation

Table 2: ST-EPR Measurements of the Effect of Chain Length on Ca-ATPase Rotational Mobility[a]

chain length	H''/H	τ_r (μS)
18	0.33	18
24	0.74	86

[a] MSL-Ca-ATPase mobility ($1/\tau_r$, μs^{-1}) was calculated from the effective correlation time, τ_r, obtained from the line shape (H''/H) as previously described (Squier & Thomas, 1986).

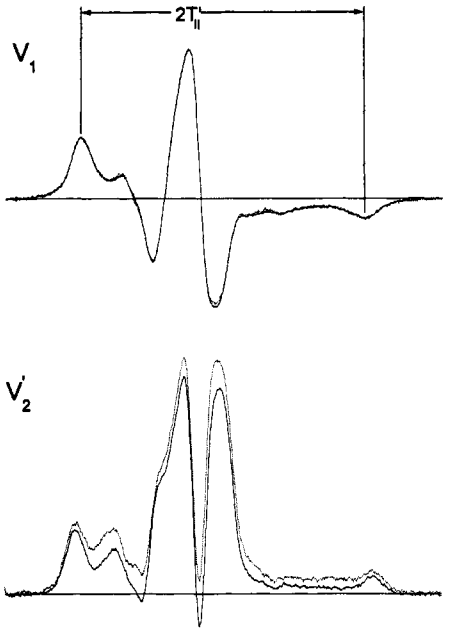

FIGURE 5: Conventional (V_1) EPR and saturation transfer (V'_2) EPR spectra of reconstituted MSL-Ca-ATPase, at 37 °C. The reconstitution lipids were 18:1 and 24:1 PCs (solid and dotted lines, respectively). Baselines represent 100 G.

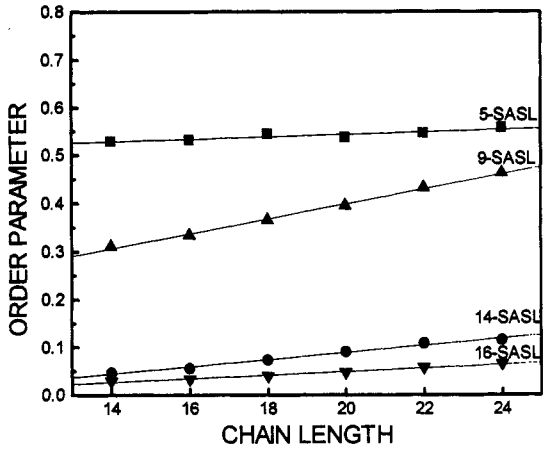

FIGURE 6: Effect of bilayer thickness on phospholipid hydrophobic chain order parameter, as determined from conventional EPR spectra of 5-, 9-, 14-, and 16-SASL incorporated into protein-free liposomes, 37 °C.

of our EPR data, it cannot account for the biphasic aspect of the activity (see below) and anisotropy dependencies on chain length.

Effect of Bilayer Thickness on the ATP-Hydrolysis Activity. The Ca^{2+}-dependent ATP hydrolysis activity of the reconstituted Ca-ATPase has a biphasic dependence on chain length (Figure 7). In agreement with Lee (1991), a maximum in activity was observed for the di(18:1)PC, while increasing inactivation occurred as the hydrophobic mismatch increased, when lipids were either too short or too long. In previous theoretical and experimental studies, it was suggested that severe deviations from an optimum bilayer thickness can cause an increase in the fraction of membrane proteins in the form of large aggregates. The dependence on chain length of the fraction of Ca-ATPase not in large aggregates—as calculated from the A_∞ values (see Discussion)—correlates with the activity dependence (Figure 7) and is supported by previous experimental evidence linking Ca-ATPase aggregation with activity inhibition.

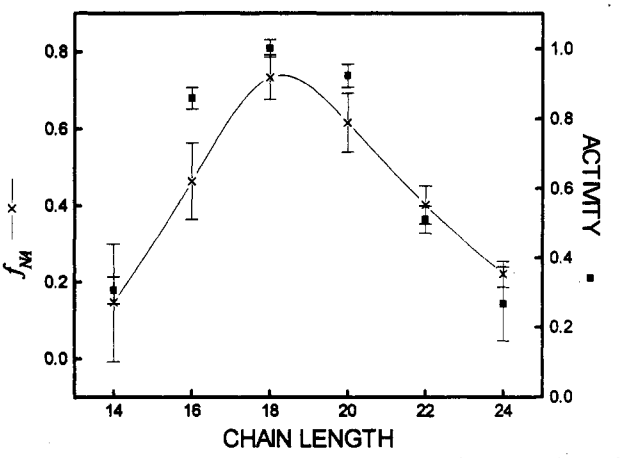

FIGURE 7: Effect of bilayer thickness on the fraction (f_{NA}) of nonaggregated protein (×) and on the ATP-hydrolysis activity (■). f_{NA} was determined from the values of residual anisotropy (A_∞). $f_{NA} = 1 - f_1$ (eq 3). The activities were normalized relative to the value for di(18:1)PC, which was 15.7 ± 1 international units. All experiments were performed at 37 °C.

Alternatively, we had to consider the possibility that irreversible denaturation was the cause for the ATPase activity effects. To determine whether this was the case, we used the nonionic detergent $C_{12}E_8$ to solubilize the reconstituted Ca-ATPase samples in which the exogenous lipid was di(14:1)-PC, di(18:1)PC, or di(24:1)PC. At the levels used here, $C_{12}E_8$ was previously found to solubilize the SR Ca-ATPase, producing lipid-free monomers (Møller et al., 1980; Andersen et al., 1986). To prevent the rapid loss of enzymatic activity found to occur during solubilization of the Ca-ATPase in $C_{12}E_8$ (Lund et al., 1989; Vilsen & Andersen, 1987), 5 mM DOPC—corresponding to a 100-fold excess relative to the lipid associated with the reconstituted protein in the assay cuvette—was present during the ATPase assays. The $C_{12}E_8$ concentration was 12 mg/mL, a saturating level for the activity effect and sufficient to clarify the phospholipid suspension. In these conditions, we detected a 1.6-fold hyperactivation [relative to the di(18:1)PC-Ca-ATPase control] of the di-(14:1)PC- and di(18:1)PC-Ca-ATPase. The activity of di-(24:1)PC-Ca-ATPase recovered to about 95% of the control value. This reversal of chain length effects on enzymatic activity by $C_{12}E_8$ rules out irreversible protein denaturation and strengthens the proposal of protein aggregation causing activity inhibition.

DISCUSSION

Hydrophobic Mismatch Causes Substantial Protein Aggregation. TPA decays of reconstituted ErITC-Ca-ATPase show that deviations of the bilayer thickness from an optimal value (d_1^0 in Figure 1) restricts microsecond rotational motion of the enzyme (Figure 3), changing primarily and consistently the normalized residual anisotropy A_∞. There are three possible explanations for this: (1) Hydrophobic mismatch could decrease the amplitude of wobble for rotation about axes in the membrane plane. However, this is unlikely to have a major effect, since previous studies have shown that Ca-ATPase rotation in native SR is dominated by uniaxial diffusion rather than wobble (Birmachu & Thomas, 1990). (2) The Ca-ATPase might have suffered denaturation during reconstitution, causing a change in probe orientation (eq 4). This cannot be ruled out, but it is unlikely, because (a) we were able to completely recover the Ca^{2+}-dependent ATPase activity (showing that no irreversible denaturation occurred) in the resolubilization experiment described above, (b) ST-

EPR results (Figure 5) are in agreement with TPA results (Figure 3), indicating significant inhibition of the rotational mobility of the Ca-ATPase (Table 2), and (c) increased protein–protein interactions are consistent with the report of elevated fluorescence energy transfer between Ca-ATPase molecules reconstituted in bilayers of suboptimal thickness (Munkonge et al., 1988). (3) The most likely explanation, which is supported by theoretical models (Mouritsen & Bloom, 1984), is an increase in the fraction f_I (eq 3) of proteins rotating on a time scale longer than the window of spectroscopic detection (500 μs in this case).

The changes in A_∞ we detected can be consistently explained on the basis of the hydrodynamic theory of Saffman and Delbrück [1975; eq 7 in this study], which predicts a loss of Ca-ATPase rotational mobility proportional to either the lipid viscosity (η), the bilayer height (h), or the protein's intramembrane surface area ($4\pi a^2$). As for the possible implication of h in the observed mobility effects, we first must highlight that this parameter refers to the actual length of contact between the integral membrane body and the bilayer. Also, X-ray diffraction data indicate a discrete transmembrane domain of Ca-ATPase about 25 Å thick (DeLong & Blasie, 1993). This means that, if h were the *only* parameter to change in eq 7, a too-thin bilayer would actually increase protein mobility, whereas a too-thick bilayer would not significantly affect protein mobility. Our data are in profound disagreement with this prediction. Therefore, the observed decrease in protein mobility must be due to an increase in either lipid viscosity or protein association.

Phospholipid Chain Dynamics Changes Only Slightly in Bilayers of Different Thickness. We selected 37 °C as our experimental temperature to ensure that all the lipids are in the liquid-crystalline phase [e.g., T_t = 26.7 °C for di(24:1cΔ^{15})PC (Lewis & Engelman, 1983b)], the homogeneity of the lipid phase being essential in order to avoid lateral segregation of proteins (occurring around T_t) into the lipid phase that best matches the protein's hydrophobic thickness (Sperotto & Mouritsen, 1991). In the case of dipalmitoylphosphatidylcholine, for example, the thickness of a fluid bilayer is 30% less than that of the gel state (Janiak et al., 1976). Previous studies in this laboratory and others have shown that membrane fluidity controls Ca-ATPase rotational mobility (Hidalgo et al., 1978; Bigelow & Thomas, 1987; Squier et al., 1988b; Birmachu & Thomas, 1990). The chain length-dependent changes in the order parameter, probed at different depths (Figure 6), are slight and do not correlate with the changes in enzyme rotational mobility and activity (Figure 7). Therefore, most of the reduced protein mobility—at longer and shorter chain lengths—must be caused by an increase in the cross-sectional area of the rotating unit in the plane of the membrane (πa^2 in eq 7), i.e., to lateral aggregation of the enzyme.

Correlation of Functional Inactivation with Protein Aggregation. Mismatch between the hydrophobic thickness of the bilayer and the hydrophobic stretch of the Ca-ATPase caused inhibition of the enzymatic activity. Inhibition occurred for lipids that were too short ($d_1 - d_1^0 < 0$) or too long ($d_1 - d_1^0 > 0$), the optimal activity being observed for 18–20-carbon phosphatidylcholines, which is similar to the optimum previously reported in studies of the same system (Lee, 1991; Johannsson et al., 1981a).

The conclusion that the primary effect of hydrophobic mismatch is to induce protein association is supported by the pattern of changes in the anisotropy amplitudes A_i (Figure 4), which should be proportional to the mole fractions f_i of populations corresponding to different aggregate sizes (Birmachu & Thomas, 1990), and A_∞, corresponding to the mole fraction of protein in large aggregates. The biphasic aspect of A_∞ (Figure 4) is mirrored with fidelity by the activity curve (Figure 7, filled squares), suggesting a direct connection between the mole fraction of protein in large aggregates and the degree of functional inactivation. On the basis of this model, the mole fraction f_{NA} of Ca-ATPase molecules *not* in large aggregates can be calculated from the residual anisotropy value as described by Birmachu and Thomas (1990), using the expression $f_{NA} = 1 - f_I = 1 - (A_\infty - A_{\infty 0})/(1 - A_{\infty 0})$. We assume that the enzyme not in large aggregates has the same $A_{\infty 0}$ (0.22) as observed in native SR microsomes, in which large-scale aggregation has been shown to be negligible (Birmachu et al., 1993). This fraction and its correlation with Ca-ATPase activity is plotted in Figure 7, indicating that most of the activity is in the mobile fraction, which is consistent with previous studies showing that enhanced protein mobility correlates with increased activity (Bigelow & Thomas, 1987), whereas enforced interactions among Ca-ATPase molecules inhibit enzymatic activity (Squier & Thomas, 1988; Squier et al., 1988a; Birmachu & Thomas, 1990; Mahaney & Thomas, 1991; Voss et al., 1991). Complete reversal of phospholipid chain length effects on enzymatic activity by detergent solubilization supports the suggestion that enzyme inactivation is indeed caused by changes in either the quaternary or tertiary structure of the Ca-ATPase and not by means of a permanent protein denaturation. The mechanism by which protein aggregation leads to inactivation is still unclear and, as previously suggested by Starling et al. (1993), it might be different for negative and positive mismatch. However, considerable evidence supports the proposal that protein mobility (i.e., lack of large-scale aggregation) is important to the enzymatic steps involving phosphoenzyme decomposition (Squier & Thomas, 1988).

Relationship to Other Experimental and Theoretical Studies. Previous reconstitution studies have established that the activity of membrane proteins can be modulated by the thickness of the surrounding phospholipid bilayer. A thickness that supports maximal activity is usually detected and is yielded by phospholipids of intermediate chain length (16–20 carbons) (Montecucco et al., 1982; In't Veld et al., 1991), similar to that observed for the SR Ca-ATPase. This observation suggests that a crucial aspect of lipid–protein interaction, or rather lipid-mediated protein–protein interaction, can be attributed to the matching between the hydrophobic transmembrane domain of the protein and the hydrophobic thickness of the lipid bilayer envelope. This hypothesis is supported by evidence of chain length-dependent protein aggregation occurring transiently (Kusumi & Hyde, 1982) or statically (Lewis & Engelman, 1983a; Ryba & Marsh, 1992) in the case of bacteriorhodopsin and rhodopsin. Indeed, protein aggregation due to hydrophobic mismatch has been speculated to occur by various theories of lipid–protein interaction, based on either phenomenological models (Owicki et al., 1978; Owicki & McConnell, 1979; Jähnig, 1981a,b; Schröder, 1977, Mouritsen & Bloom, 1984) or microscopic statistical mechanical analysis (Marčelja, 1976; Pink & Chapman, 1979; Tessier-Lavigne et al., 1982). These theories predict lateral segregation to occur for small transmembrane peptides, but only as a consequence of a rather large mismatch between the protein hydrophobic span and the phospholipid hydrophobic thickness. The large cytosolic moiety, characteristic of numerous integral membrane proteins including the SR Ca-ATPase (Stokes & Green, 1990), is proposed to

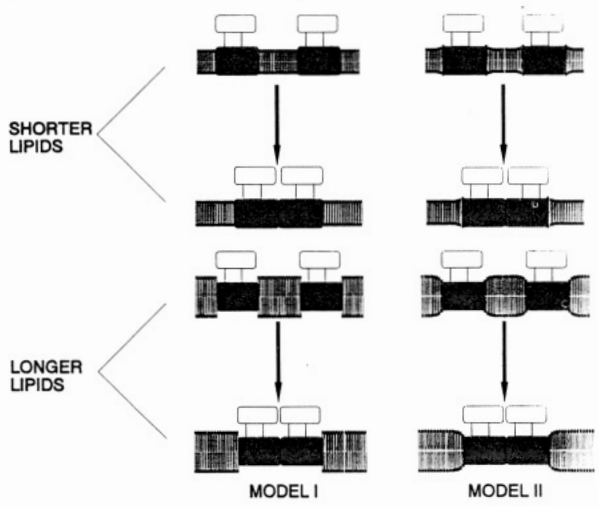

FIGURE 8: Schematic representation of the two situations tested in our experiments: (A) bilayer too thin, (B) bilayer too thick. We propose two mechanisms that can account for protein aggregation in mismatched membranes: (I) The membrane protein must aggregate in order to minimize lipid–protein interfaces, and therefore the energetically unfavorable exposure of hydrophobic surfaces to the aqueous environment. (II) The phospholipid hydrocarbon chains must stretch or compress at lipid–protein interfaces to avoid exposure of hydrophobic surfaces to the hydrophilic environment. The resulting increased strain is reduced by aggregating the proteins in order to minimize the energetically unfavorable lipid–protein contacts.

add a protein-specific contribution, possibly by enhancing the tendency toward aggregation. This may explain the intriguing contrast in the response to hydrophobic mismatch observed in the closely related Ca-ATPase and Na,K-ATPase. The enzymatic activity as a function of chain length has a much sharper maximum for the Ca-ATPase than for the Na,K-ATPase, which shows a broad plateau between 16- and 20-carbon lipids (Johannsson et al., 1981b).

Models for the Mismatch-Induced Protein Aggregation. The above results suggest that the hydrophobic mismatch leads to Ca-ATPase inhibition primarily by inducing the formation of large-scale aggregates of Ca-ATPase molecules. One can envisage large-scale aggregation of proteins occurring as a means for minimizing the free energy of interaction between the integral membrane protein and the phospholipid bilayer envelope. For a nonzero hydrophobic mismatch ($d_p - d_1^0 \neq 0$, Figure 1), aggregation may occur as a tendency of the system to minimize the unfavorable exposure of hydrophobic surfaces (either transmembrane parts of the protein or lipid hydrocarbon chains) to a hydrophilic environment (the cytosol). In an extreme case, the protein embedded in a *rigid* mismatched bilayer (Figure 8, model I) must aggregate in order to minimize protein–lipid interfaces where hydrophobic surfaces would be unavoidably exposed. In model II (Figure 8)—which has been recently theorized by Fattal and Ben-Shaul (1993)—the bilayer thickness is perturbed by either stretching or compressing the phospholipid hydrophobic chains in order to adjust to the optimal thickness (d_1^0) required by the protein. While stretching the lipids results in an unfavorable loss of entropy, compressing them might also have a more subtle unfavorable contribution to the free energy of lipid–protein interaction. There is abundant physical evidence that the Ca-ATPase of the sarcoplasmic reticulum undergoes a series of conformational changes as the enzyme proceeds through its reaction cycle. It has been suggested that these protein conformational states might require different bilayer thicknesses (Michelangeli et al., 1990; Starling et al., 1993), such that artificially perturbing the bilayer thickness could actually be a way of altering the protein's conformational equilibrium. This is supported by evidence of small distortions of α-helical conformation of small peptides occurring in certain conditions as a consequence of mismatch (Zhang et al., 1992), suggesting that changes in the equilibrium constants of enzyme states require subtle alterations of the secondary or tertiary structure. Despite indications that protein aggregation is the most likely effect of hydrophobic mismatch, it is possible that the changes in residual anisotropy we measure are the effect of probe reorientation, which cannot be distinguished from probe immobilization.

Conclusions. Although severe perturbations of bilayer thickness in natural membranes are unlikely to occur, their manipulation in reconstitutions of the SR Ca pump have proven an excellent technique for confirming theoretical projections about molecular dynamics. Our experiments confirm that hydrophobic mismatch causes aggregation of the Ca-ATPase as predicted by theoretical models. Furthermore, we propose that it is by inducing the formation of large-scale protein aggregates that mismatch causes inhibition of the reconstituted enzyme. The profile of lipid chain dynamics cannot be responsible for our activity results. Future studies should be directed toward defining the mechanism by which aggregation causes inhibition.

ACKNOWLEDGMENT

We thank Joseph Mersol, Richard Stein, and John Voss for helpful discussions and Robert Bennett, Franz Nisswandt, and Nicoleta Cornea for technical assistance. We thank James Mahaney for critically reading the manuscript. We are especially thankful for the technical advice provided by Anthony Lee in the initial phase of this project.

REFERENCES

Andersen, J. P., Vilsen, B., Nielsen, H., & Møller, J. V. (1986) *Biochemistry 25*, 6439–6447.
Bigelow, D. J., & Thomas, D. D. (1987) *J. Biol. Chem. 262*, 13449–13456.
Bigelow, D. J., & Inesi, G. (1991) *Biochemistry 30*, 2113–2125.
Bigelow, D. J., Squier, T. C., & Thomas, D. D. (1986) *Biochemistry 25*, 194–202.
Birmachu, W., & Thomas, D. D. (1990) *Biochemistry 29*, 3904–3914.
Birmachu, W., Voss, J. C., Louis, C. F., & Thomas, D. D. (1993) *Biochemistry 32*, 9445–9453.
Chen, P. S., Toribara, T. Y., & Warner, H. (1956) *Anal. Chem. 28*, 1756–1758.
Criado, M., Eibl, H., & Barrantes, F. J. (1984) *J. Biol. Chem. 259*, 9188–9198.
DeLong, L. J., Blasie, J. K. (1993) *Biophys J. 64*, 1750–1759.
Eads, T. M., Thomas, D. D., & Austin, R. H. (1984) *J. Mol. Biol. 179*, 55–81.
East, J. M., & Lee, A. G. (1982) *Biochemistry 21*, 4144–4151.
Fattal, D. R., & Ben-Shaul, A. (1993) *Biophys. J. 65*, 1795–1809.
Fernandez, J. L., Rosemblatt, M., & Hidalgo, C. (1980) *Biochim. Biophys. Acta 599*, 552–568.
Froud, R. J., East, J. M., Jones, O. T., & Lee, A. G. (1986) *Biochemistry 25*, 7544–7552.
Gaffney, B. J. (1976) in *Spin Labeling Theory and Practice* (Berliner, L. J., Ed.) pp 567–571, Academic Press, New York.
Gornall, A. G., Bardawill, C. J., & David, M. M. (1949) *J. Biol. Chem. 177*, 751–766.
Hidalgo, C., Thomas, D. D., & Ikemoto, I. (1978) *J. Biol. Chem. 253*, 6879–6887.
In't Veld, G., Driessen, A. J. M., Op den Kamp, J. A. F., & Konings, W. N. (1991) *Biochim. Biophys. Acta. 1065*, 203–212.

Jähnig, F. (1981a) *Biophys. J. 36*, 329–345.
Jähnig, F. (1981b) *Biophys. J. 36*, 347–357.
Janiak, M. J., Small, D. M., & Shipley, G. G., (1976) *Biochemistry 15*, 4575–4580.
Johannsson, A., Keightley, C. A., Smith, G. A., Richards, C. D., Hesketh, T. R., & Metcalfe, J. C. (1981a) *J. Biol. Chem. 256* (4), 1643–1650.
Johannsson, A., Smith, G. A., & Metcalfe, J. C. (1981b) *Biochim. Biophys. Acta 641*, 416–421.
Karon, B. S., & Thomas, D. D. (1993) *Biochemistry 32*, 7503–7511.
Kinosita, K., Ishiwata, S., Yoshimura, H., Asai, H., & Ikegami, A. (1984) *Biochemistry 23*, 5963–5975.
Kusumi, A., & Hyde, J. S., (1982) *Biochemistry 21*, 5978–5983.
Lee, A. G., (1991) *Prog. Lipid. Res 30* (4) 323–348.
Lewis, B. A., & Engelman, D. M. (1983a) *J. Mol. Biol. 166*, 203–210.
Lewis, B. A., & Engelman, D. M. (1983b) *J. Mol. Biol. 166*, 211–217.
Lewis, S. M., & Thomas, D. D. (1986) *Biochemistry 25*, 4615–4621.
Lipari, G., & Szabo, A. (1980) *Biophys. J. 30*, 489–506.
Ludescher, R. D., & Thomas, D. D. (1988) *Biochemistry 27*, 3343–3351.
Lund, S., Orlowski, S., de Foresta, B., Champeil, O., le Maire, M., & Møller, J. P. (1989) *J. Biol. Chem. 264* (9), 4907–4915.
Mahaney, J. E., & Thomas, D. D. (1991) *Biochemistry 30*, 7171–7180.
Marčelja, S. (1976) *Biochim. Biophys. Acta*, 367, 165–176.
Michelangeli, F., Orlowski, S., Champeil, P., Grimes, E. A., East, J. M., & Lee, A. G. (1990) *Biochemistry 29*, 8307–8312.
Montecucco, C., Smith, G. A., Dabbeni-sala, F., Johannsson A., Galante, Y. M., & Bisson, R. (1982) *FEBS Lett. 144* (1), 145–148.
Møller, J. V., Lind, K. E., & Andersen, J. P. (1980) *J. Biol. Chem. 255* (5), 1912–1920.
Mouritsen, O. G., & Bloom, M. (1984) *Biophys. J. 46*, 141–153.
Munkonge, F., Michelangeli, F., Rooney, E. K., East, J. M., & Lee, A. G. (1988) *Biochemistry 27*, 6800–6805.
Owicki, J. C., & McConnell, H. M. (1979) *Proc. Natl. Acad. Sci. U.S.A. 76*, 4750–4754.
Owicki, J. C., Springgate, M. W., & McConnell, H. M. (1978) *Proc. Natl. Acad. Sci. U.S.A. 75*, 1616–1619.
Pink, D. A., & Chapman, D. (1979) *Proc. Natl. Acad. Sci. U.S.A. 76*, 1542–1546.
Popp, C. A., & Hyde, J. S. (1981) *J. Magn. Reson. 43*, 249–258.
Ryba, N. J. P., & Marsh, D. (1992) *Biochemistry 31*, 7511–7518.
Saffman, P. J., & Delbrück, M. (1975) *Proc. Natl. Acad. Sci. U.S.A. 72*, 3111–3113.
Schröder, H. (1977) *J. Chem. Phys. 657*, 1617–1619.
Sperotto, M. M., & Mouritsen, O. G. (1991) *Eur. Biophys. J. 19*, 157–168.
Squier, T. C., & Thomas, D. D. (1986) *Biophys. J. 49*, 921–935.
Squier, T. C., & Thomas, D. D. (1988) *J. Biol. Chem. 263*, 9171–9177.
Squier, T. C., & Thomas, D. D. (1989) *Biophys. J. 56*, 735–748.
Squier, T. C., Hughes, S. E., & Thomas, D. D. (1988a) *J. Biol. Chem. 263*, 9162–9170.
Squier, T. C., Bigelow, D. J., & Thomas, D. D. (1988b) *J. Biol. Chem. 263*, 9178–9186.
Starling, A. P., East, J. M., & Lee, A. G. (1993) *Biochemistry 32*, 1593–1600.
Stokes, D. L., & Green, N. M. (1990) *Biophys. J. 57*, 1–14.
Tessier-Lavigne, M., Boothroyd, A., Zuckerman, M. J., & Pink, D. A. (1982) *J. Chem. Phys. 76*, 4587–4599.
Thomas, D. D. (1986) in *Techniques for the Analysis of Membrane Proteins* (Ragan, C. I., & Cherry, R. J., Eds.) pp 377–431, Chapman and Hall, London.
Thomas, D. D., & Hidalgo, C. (1978) *Proc. Natl. Acad. Sci. U.S.A. 75*, 5488–5492.
Thomas, D. D., & Mahaney, J. E. (1993) in *New Comprehensive Biochemistry: Lipid–Protein Interactions* (Watts, A., Ed.) pp 301–320, Elsevier, Amsterdam.
Voss, J., Hussey, D., Birmachu, W., & Thomas, D. D. (1991) *Biochemistry 30*, 74948–7506.
Vilsen, B., & Andersen, J. P. (1987) *Eur. J. Biochem. 170*, 421–429.
Zhang, Y.-P., Lewis, R. N. A. H., Hodges, R. S., & McElhaney, R. N. (1992) *Biochemistry 31*, 11579–11588.